

Supplementary Information:

Significant differences of monooxotungsten(IV) and dioxotungsten(VI) benzenedithiolates containing two intramolecular NH···S hydrogen bonds from molybdenum analogues

Taka-aki Okamura,* Yui Omi, Manami Fujii, Miki Tatsumi and Kiyotaka Onitsuka

Department of Macromolecular Science, Graduate School of Science, Osaka University, Toyonaka,
Osaka 560-0043, Japan

E-mail: tokamura@chem.sci.osaka-u.ac.jp

Table S1 Crystallographic data for (NEt₄)₂[W^{IV}O(1,2-S₂-3-*t*-BuNHCOC₆H₃)₂] (**1-W**), (NEt₄)₂[W^{IV}(1,2-S₂-3-*t*-BuNHCOC₆H₃)₃]·H₂O (**3·H₂O**), and (NEt₄)₂[{W^{VI}O₂(1,2-S₂-3-*t*-BuNHCOC₆H₃)₂(μ-O)]·2(Et₂O) (**4·2(Et₂O)**)

	1-W	3·H₂O	4·2(Et₂O)
empirical formula	C ₃₈ H ₆₆ N ₄ O ₃ S ₄ W	C ₄₉ H ₈₁ N ₅ O ₄ S ₆ W	C ₄₆ H ₈₆ N ₄ O ₉ S ₄ W ₂
formula weight	939.04	1180.39	1335.12
color	orange	red	yellow
crystal system	orthorhombic	orthorhombic	monoclinic
<i>a</i> , Å	8.865(2)	21.3866(5)	17.9606(14)
<i>b</i> , Å	16.289(3)	18.6641(4)	8.7047(8)
<i>c</i> , Å	29.929(7)	29.515(2)	18.3212(14)
<i>β</i> , deg	90	90	91.438(5)
<i>V</i> , Å ³	4321.8(16)	11781.4(9)	2863.5(4)
space group	<i>P</i> 2 ₁ 2 ₁ 2 ₁	<i>Pna</i> 2 ₁	<i>P</i> 2 ₁ / <i>c</i>
<i>Z</i>	4	8	2
<i>D</i> _{calc} , g/cm ³	1.443	1.331	1.548
<i>F</i> (000)	1936	4896	1348
<i>μ</i> (MoKα), mm ⁻¹	2.905	2.216	4.210
Scan type	ω	ω	ω
2θ _{max} , deg	50	50	55
No. of Reflections unique	7323	20684	6532
No. Variables	454	1172	295
residuals; <i>R</i> 1 ^{<i>a</i>} (<i>I</i> > 2σ(<i>I</i>)), <i>wR</i> 2 ^{<i>b</i>}	0.0685, 0.1540	0.0781, 0.1503	0.0293, 0.0437
(all data)			
GOF	1.199	1.113	0.858

$${}^a R1 = \sum ||F_o| - |F_c|| / \sum |F_o|. \quad {}^b wR2 = \{ \sum [w(F_o^2 - F_c^2)^2] / \sum [w(F_o^2)^2] \}^{1/2}$$

Table S2 Raman bands of monooxo-tungsten and molybdenum complexes

Complex	<i>ν</i> (M=O)/cm ⁻¹	References
(NEt ₄)[W ^V O(SC ₆ F ₅) ₄]	980	This work
(NEt ₄)[W ^V O(SPh) ₄]	943 ^{<i>a</i>}	12
(NEt ₄)[Mo ^V O(SC ₆ F ₅) ₄]	982 ^{<i>a</i>}	30
(NEt ₄)[Mo ^V O(SPh) ₄]	936	38
(NEt ₄) ₂ [W ^{IV} O(SC ₆ F ₅) ₄]	949	This work
(HNEt ₃) ₂ [Mo ^{IV} O(SC ₆ F ₅) ₄]	927 ^{<i>a</i>}	30

^{*a*}IR spectra.

Table S3 Chemical shifts and proposed structures of **LH₂** and the deprotonated forms in acetonitrile-*d*₃

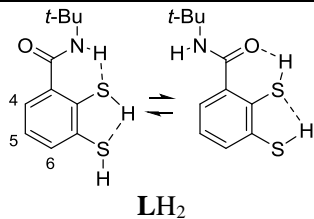
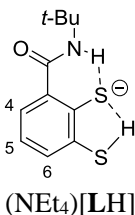
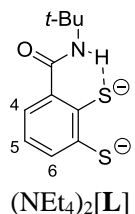
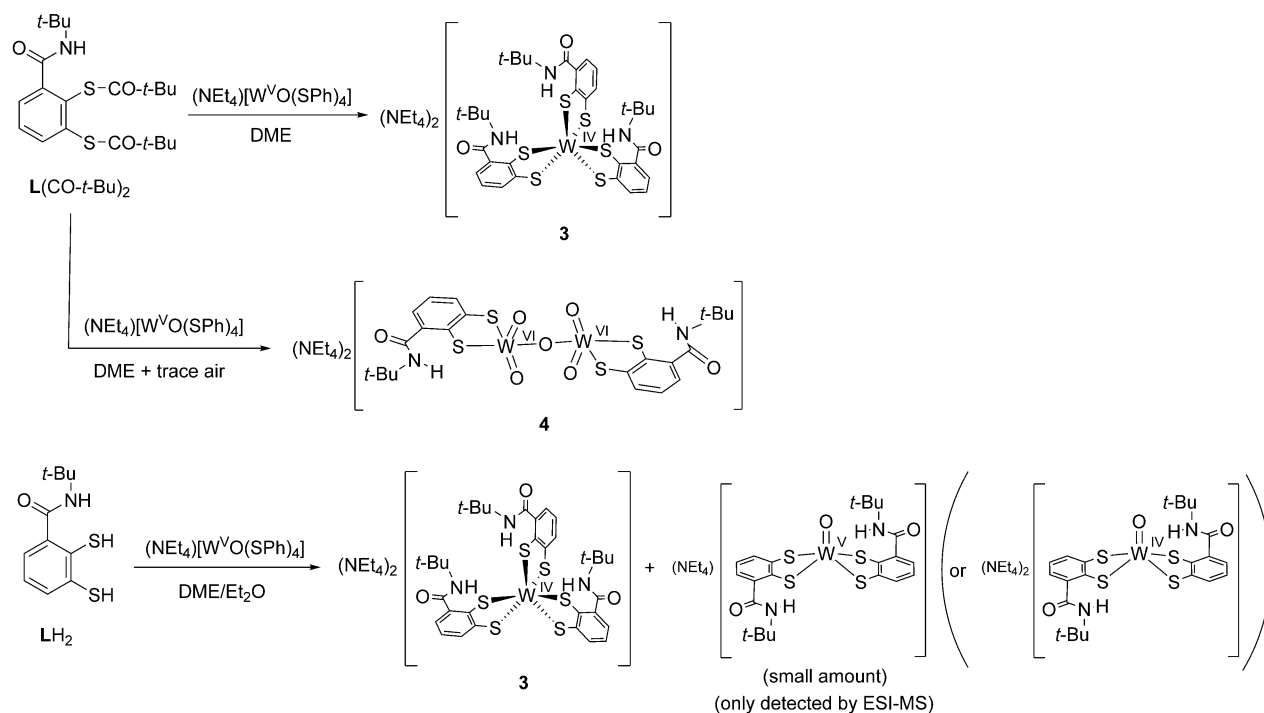
	4-H (dd)	6-H (dd)	5-H (t)	NH (br s)	SH (br s)	<i>t</i> -Bu (s)
 <p>LH₂</p>	7.42	7.23	7.05	6.85	5.00	1.41
 <p>(NEt₄)[LH]</p>	7.72	7.33	6.57	11.78	9.01	1.43
 <p>(NEt₄)₂[L]</p>	7.78	7.04	6.58	12.21		1.45

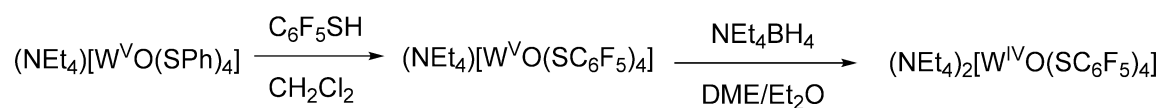
Table S4 Contributions of NH...S hydrogen bonds to W and Mo complexes

			W	Mo ^e
1-M	X-ray	$\Delta(M=O)^a/\text{\AA}$	-0.012(9)	-0.001(6)
		$\Delta(M-S)^a/\text{\AA}$	-0.028(4) — -0.001(4)	-0.040(2) — -0.003(2)
			(mean -0.012(4))	(mean -0.019(4))
	IR	$\Delta\nu(\text{NH})^b/\text{cm}^{-1}$	-191	-198
		$\Delta\nu(M=O)^a/\text{cm}^{-1}$	+15	+13
CV	$\Delta E_{1/2}^a/V$	+0.15	+0.12	
2-M	IR	$\Delta\nu(\text{NH})^d/\text{cm}^{-1}$	-206	-209
	Raman	$\Delta\nu_s(M=O)^c/\text{cm}^{-1}$	+9	+13
		$\Delta\nu_{as}(M=O)^c/\text{cm}^{-1}$	+13	+11

^aDifference of the values between **1-M** and (NEt₄)₂[M^{IV}O(bdt)] (**5-M**). (W=O, 1.727(2) Å; W-S, 2.372(4) Å for (NEt₄)₂[W^{IV}O(bdt)₂] (**5-W**);¹⁴ Mo=O, 1.699(6) Å; Mo-S, 2.388(2) Å for (NEt₄)₂[Mo^{IV}O(bdt)₂] (**5-Mo**).⁵⁰ ^bSee Table 3. ^cDifference of the values between **2-M** and (NEt₄)₂[M^{VI}O₂(bdt)₂] (**6-M**). ^dSee Table 4. ^eRef. 29.



Scheme S1 Reaction of $(\text{NEt}_4)[\text{W}^{\text{V}}\text{O}(\text{SPh})_4]$ with LH_2 or $\text{L}(\text{CO-}t\text{-Bu})_2$ according to the molybdenum analogue.



Scheme S2 Preparation of $(\text{NEt}_4)_2[\text{W}^{\text{IV}}\text{O}(\text{SC}_6\text{F}_5)_4]$.

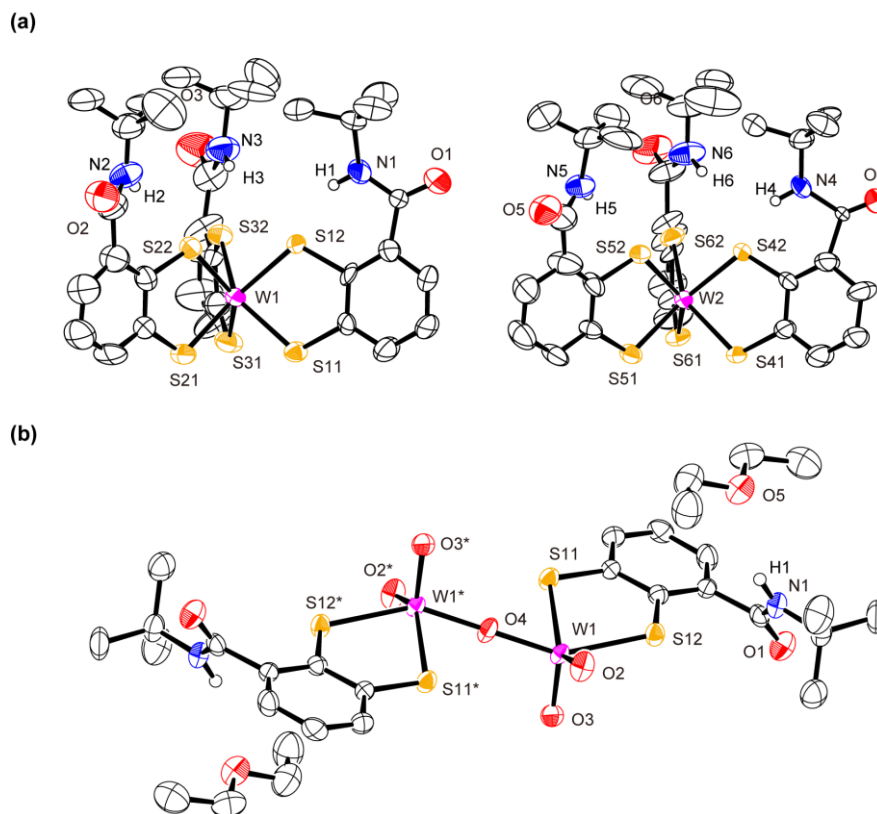


Fig. S1 Molecular structures (anion parts) of (a) $(\text{NEt}_4)_2[\text{W}^{\text{IV}}(1,2\text{-S}_2\text{-3-}t\text{-BuNHCOC}_6\text{H}_3)_3]$ (**3**) and (b) $(\text{NEt}_4)_2\{[\text{W}^{\text{VI}}\text{O}_2(1,2\text{-S}_2\text{-3-}t\text{-BuNHCOC}_6\text{H}_3)]_2(\mu\text{-O})\}$ (**4**) in the crystal. Two molecules of **3** were found in the asymmetric unit.

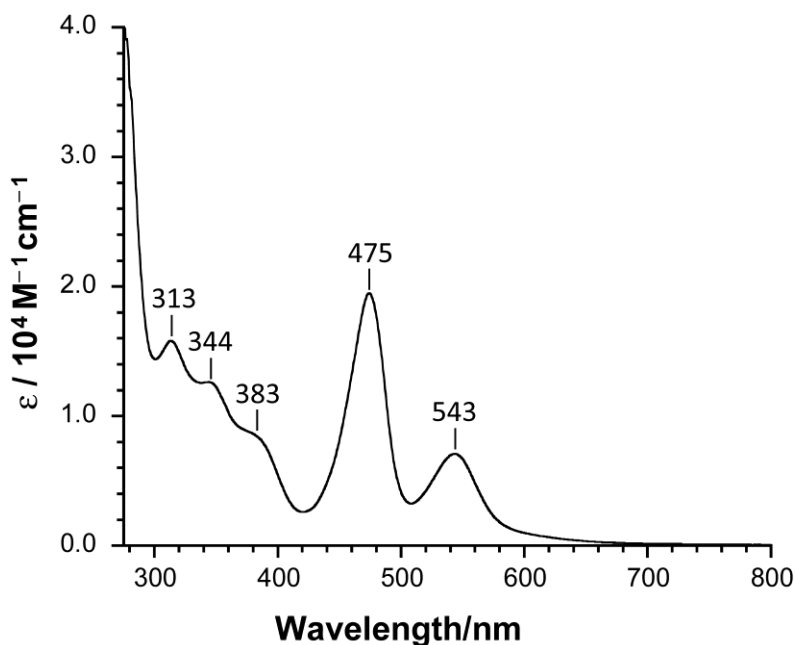


Fig. S2 UV-vis spectrum of $(\text{NEt}_4)_2[\text{W}^{\text{IV}}(1,2\text{-S}_2\text{-3-}t\text{-BuNHCOC}_6\text{H}_3)_3]$ (**3**) in DMF.

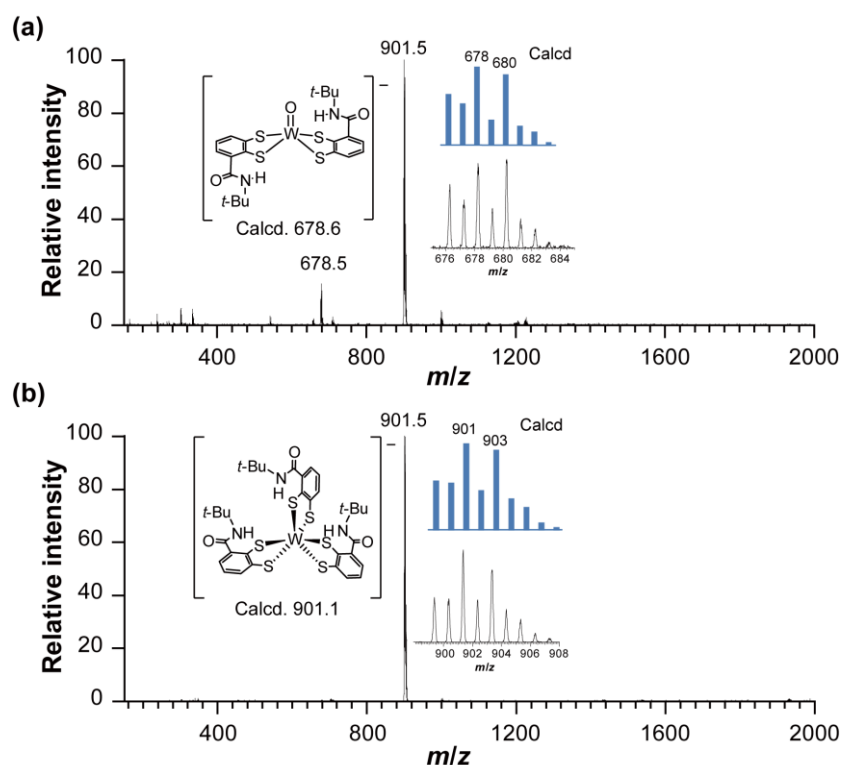


Fig. S3 ESI-MS spectra of (a) the products in DME/Et₂O shown in Scheme S1, where the main peak was (NEt₄)₂[W^{IV}(1,2-S₂-3-*t*-BuNHCOC₆H₃)₃] (**3**) and a small amount of (NEt₄)[W^{VO}O(1,2-S₂-3-*t*-BuNHCOC₆H₃)₂] was found, and (b) pure **3**. The enlarged spectra were obtained in the zoom scan mode, accompanying simulated isotope patterns.

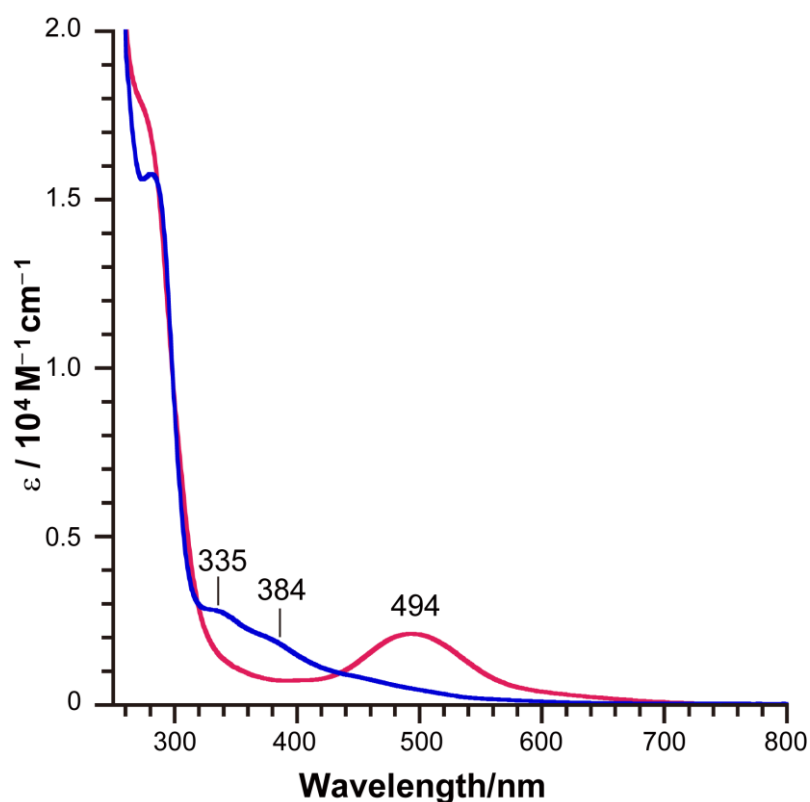


Fig. S4 UV-vis spectra of (NEt₄)[W^{VO}O(SC₆F₅)₄] (red line) in acetonitrile and (NEt₄)₂[W^{IV}O(SC₆F₅)₄] (blue line) in DMF.

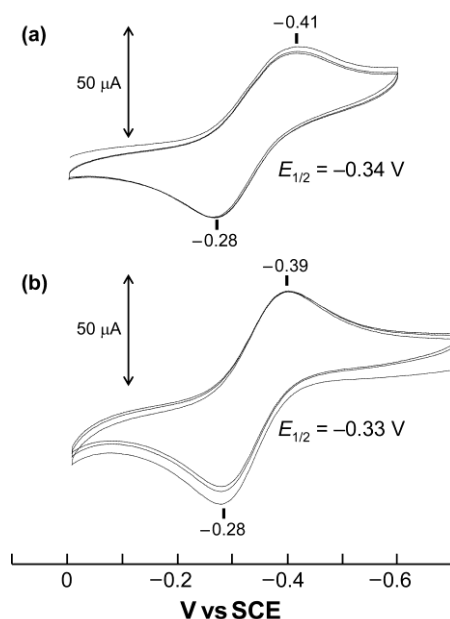


Fig. S5 Cyclic voltammograms of (a) $(\text{NE}_4)[\text{W}^{\text{V}}\text{O}(\text{SC}_6\text{F}_5)_4]$ and (b) $(\text{NE}_4)_2[\text{W}^{\text{IV}}\text{O}(\text{SC}_6\text{F}_5)_4]$ in DMF.

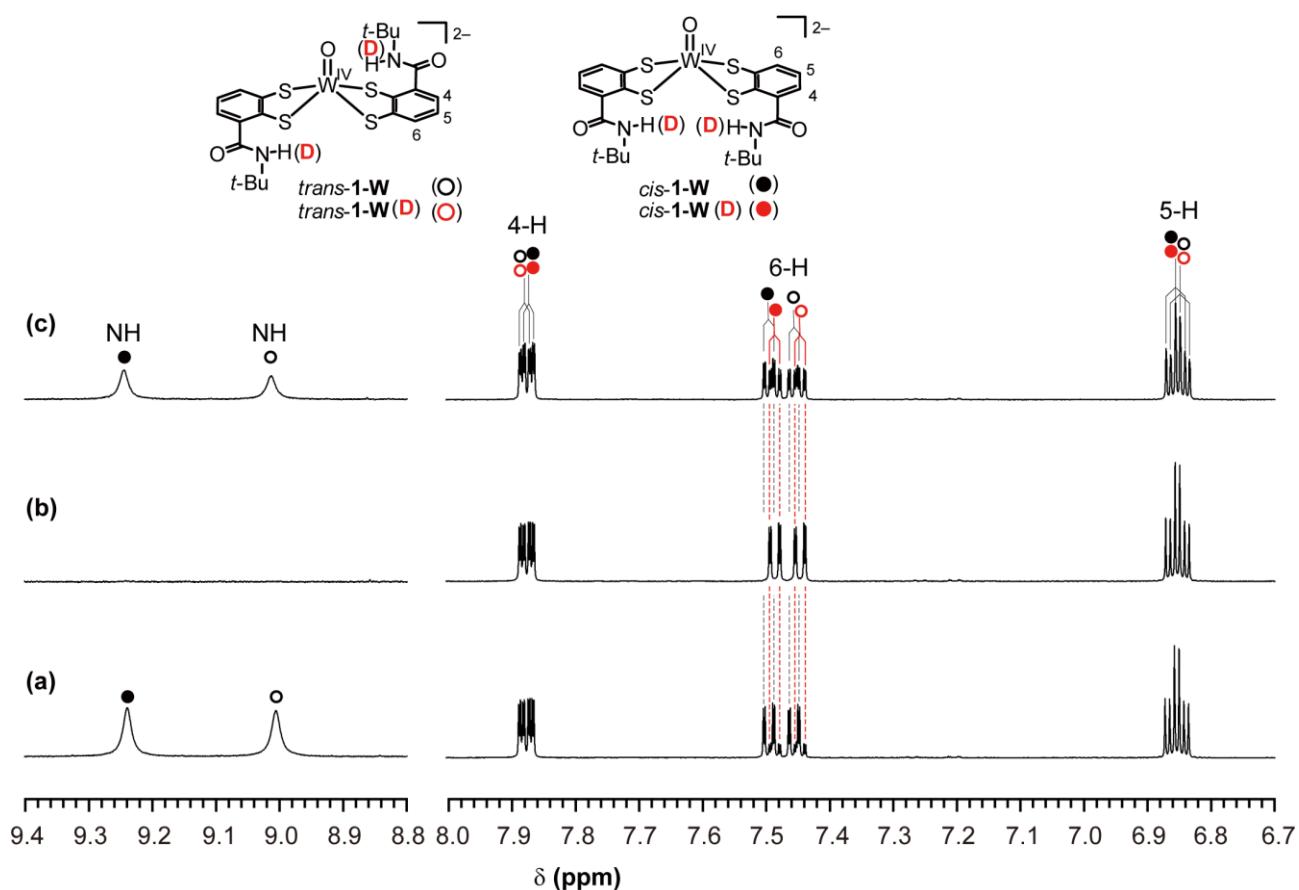


Fig. S6 ^1H NMR spectra (measured at $30\text{ }^\circ\text{C}$) of (a) $(\text{NE}_4)_2[\text{W}^{\text{IV}}\text{O}(1,2\text{-S}_2\text{-3-}t\text{-BuNHCOC}_6\text{H}_3)_2]$ (**1-W**, *trans/cis* = 1:1) containing a minute amount of NE_4BH_4 in acetonitrile- d_3 , (b) after heating at $50\text{ }^\circ\text{C}$ for 30 min., and (c) after addition of a trace amount of H_2O . The content of $(\text{NE}_4)_2[\text{W}^{\text{IV}}\text{O}(1,2\text{-S}_2\text{-3-}t\text{-BuNDCOC}_6\text{H}_3)_2]$ (**1-W(ND)**) was increased from (a) 22% to (b) 93%, and then back to about 50% by the addition of H_2O . The 4-H and 5-H signals of **1-W** and **1-W(ND)** were found at identical chemical shifts for each isomer.

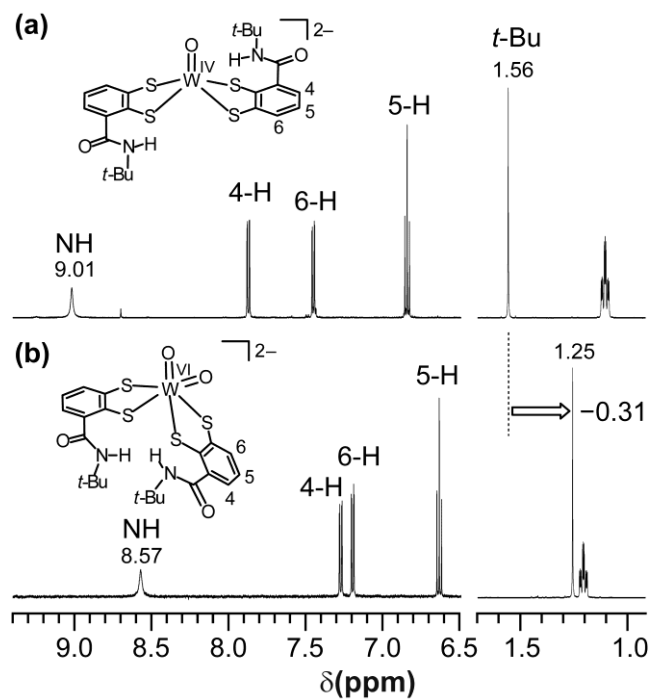


Fig. S7 ^1H NMR spectra of (a) $(\text{NEt}_4)_2[\text{W}^{\text{IV}}\text{O}(1,2\text{-S}_2\text{-3-}t\text{-BuNHCOC}_6\text{H}_3)_2]$ (**1-W**) and (b) $(\text{NEt}_4)_2[\text{W}^{\text{VI}}\text{O}_2(1,2\text{-S}_2\text{-3-}t\text{-BuNHCOC}_6\text{H}_3)_2]$ (**2-W**) in acetonitrile- d_3 at 30 °C. The aromatic region was enlarged along vertical axis.

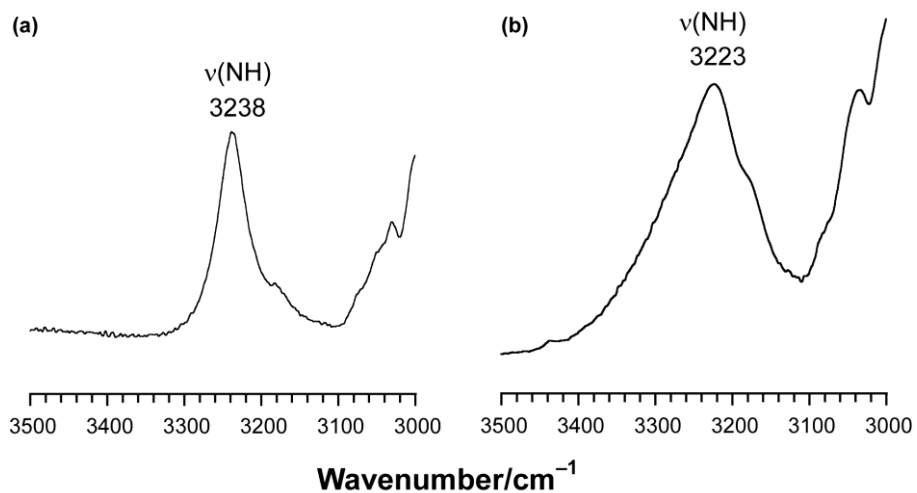


Fig. S8 IR spectra of (a) $(\text{NEt}_4)_2[\text{W}^{\text{IV}}\text{O}(1,2\text{-S}_2\text{-3-}t\text{-BuNHCOC}_6\text{H}_3)_2]$ (**1-W**) and (b) $(\text{NEt}_4)_2[\text{W}^{\text{VI}}\text{O}_2(1,2\text{-S}_2\text{-3-}t\text{-BuNHCOC}_6\text{H}_3)_2]$ (**2-W**) in the solid state.

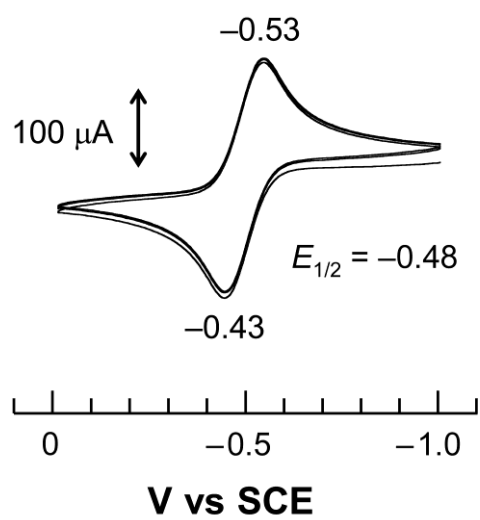


Fig. S9 Cyclic voltammogram of $(\text{NEt}_4)_2[\text{W}^{\text{IV}}\text{O}(\text{1,2-S}_2\text{-3-}t\text{-BuNHCOC}_6\text{H}_3)_2]$ (**1-W**) in DMF.